JOURNAL OF GEOPHYSICAL RESEARCH, VOL. 102, NO. B12, PAGES 27,367–27,377, DECEMBER 10, 1997

Model quakes in the two-dimensional wave equation

Bruce E. Shaw

Lamont-Doherty Earth Observatory, Columbia University, Palisades, New York

Abstract. This paper presents a new two-dimensional wave equation model of an earthquake fault. The model generates a complex sequence of slip events on a fault with uniform properties when there is a frictional weakening instability. Previous models of long faults in one and two dimensions had the driving in the bulk, giving the Klein-Gordon equation in the bulk. Here, I place the driving on the boundary, giving the wave equation in the bulk. The different models are, however, shown to behave similarly. I examine a whole range of frictions, with slip weakening as one end-member case and velocity weakening as the other end-member case, and show that they display a generic type of slip complexity: there is an exponential distribution of the largest events and, for sufficient weakening, a power law distribution of small events. With the addition of a viscous-type friction term on the fault, I show that the results are independent of grid resolution, indicating that continuum limit complexity is achieved.

1. Introduction

Earthquakes are complex in many ways. The distribution of slip along the fault, the radiated waves that are emitted, and the timing and correlation between events are just some of the ways that earthquakes exhibit complexity. Not only are earthquakes complex, but the faults on which earthquakes occur are themselves complex. Faults are parts of whole systems of faults which accommodate deformation. Faults themselves are not simple linear features but have bends, steps, jogs, and even smaller-scale roughness. Across the fault there is structure as well, from gouge to breccia to rock. As well, along the faults there are different types of rocks. And these are just the relatively static features of a fault that evolve over geological time. During earthquakes, a whole slew of processes, such as interactions with fluids, to mention just one, evolve on quite rapid timescales. How does one even begin to try to deal with such a complicated system?

One approach has been to start with the simplest system, try to understand how this system behaves, and then, piece by piece, systematically add in more complications. This has the advantage of helping to separate which ingredients are affecting which outcomes. Simplifying the problem in this manner is not only useful but necessary: even if one wanted to try to include everything, current computers would not be capable of solving the complete systems. Hence one has to simplify things.

The simplest elastodynamic model of a fault was presented by *Burridge and Knopoff* [1967], who described a one-dimensional model. *Carlson and Langer* [1989] showed that with an appropriate frictional instability, the one-dimensional models could develop complexity dynamically, even in the case where the fault itself had completely uniform properties. They observed a power law distribution of small events and an excess of large events that occurred above the extrapolated small event rate. A variety of earthquake-like properties have been observed in the simple one-dimensional model, including a cycle of small event activity preceding large events [*Shaw et al.*, 1992] and moment source spectra consistent with real earthquakes [*Shaw*, 1993].

Despite the impressive array of behaviors exhibited in one dimension, there were a number of features missing in one dimension: stress concentrations do not develop as they do in higher dimensions, and there is no radiated elastic energy. Questions remained as to whether this complexity would persist when the model was extended to higher dimensions to include long-range elastic interactions. This question was answered recently in a two-dimensional extension which showed that, indeed, dynamic complexity was produced on a uniform fault [*Myers et al.*, 1996]. In *Myers et al.* [1996]'s model, the loading was placed in the bulk, so that, as in the one-dimensional model, a Klein-Gordon equation for the bulk was obtained. A different two-dimensional geometry was considered by *Cochard and Madariaga* [1996] and *Nielsen et al.* [1995], who considered a finite fault which was pinned at the ends in unbreakable barriers. This gave a two-dimensional wave equation for the bulk. This geometry is limited, however, to short faults, where the fault length is less that the width of the seismogenic zone. Thus the large events in this geometry break or scale with the whole fault length and are controlled by this imposed geometry. Further, since faults are not allowed to grow, stress singularities develop at the unbreakable ends. *Rice and Ben-Zion* [1996] considered a

Paper number 97JB02786.
0148-0227/97/97JB-02786$09.00

two-dimensional geometry where only the depth direction was retained; thus the length of the fault was again limited to the width of the seismogenic zone.

In this paper, I present an alternative two dimensional model in which the loading occurs on a boundary which is away from, and parallel to, the fault. In this way, as did *Myers et al.* [1996], I construct a fault which is valid for arbitrary lengths, but now the equation for the bulk is the two-dimensional wave equation. I compare the results of these two different loading geometries and, nevertheless, show that they behave essentially the same way.

To specify the model, not only the geometry of the fault is needed, but also the friction along the fault. In this paper I show that a whole range of frictions, with slip weakening as one end-member case and velocity weakening as the other end-member case, display a generic type of slip complexity: The largest events are distributed exponentially, and for sufficient weakening, the small events show a power law distribution. With the addition of a viscous-type friction term on the fault to stabilize the smallest scales, I show that the results are independent of grid resolution, indicating that continuum limit complexity is achieved.

The existence of complexity in the small events has been the subject of much discussion in the literature. In addition to the different geometries the different groups have used, different frictions have been used, and different results have been obtained. *Nielsen et al.* [1995] did not see complexity, using a friction with only a time dependent drop and neither slip nor velocity weakening. *Rice and Ben-Zion* [1996], using a laboratory-based friction with a single logarithmic weakening also did not see small event complexity. *Myers et al.* [1996], using a small time dependent drop and slip weakening friction, saw complexity in the small events. *Cochard and Madariaga* [1996], using highly velocity weakening friction, also saw some complexity in the small events. Sorting out to what extent these differences in results arise from differences in friction, or from differences in geometry, is an important and unresolved question. Toward this end, I study the same friction in two different long fault geometries; interestingly, I get very similar results, thus showing a genericness in the response to the friction which transcends at least some aspects of geometry.

The rest of the paper is organized as follows. In section 2, I present the model and discuss the friction used. The results of the numerical simulation follow in section 3. I conclude in section 4.

2. The Model

The simplified picture of a fault we have in mind, which I will even further simplify, is as follows. The fault is a planar surface on an elastic bulk which is slowly, uniformly, loaded. Friction on the fault plays a central role in the problem. At depth, below the seismogenic zone, there is frictional strengthening, and the fault slides stably, creeping along at the slow plate loading rate. At seismogenic depths, there is frictional weakening, and the fault slides unstably in sudden stick-slip events [*Brace and Byerlee*, 1966; *Blanpied et al.*, 1991]. The coupling of the stuck seismogenic fault to the lower stably sliding creeping region loads the stuck fault. It also ties the displacement field to a reference field, which then constrains the maximum amount of slip when the whole seismogenic depth ruptures in a large event. This coupling is neglected in the short-fault models.

The two-dimensional model we consider simplifies this picture by treating the long two-dimensional seismogenic fault surface as a long one-dimensional line, treating the creeping lower fault as a separate parallel one-dimensional line, and connecting the two by a scalar elastic field. Thus the model consists of an elastodynamic bulk, along with boundary conditions, with the fault being a frictional weakening boundary. In this paper, we consider the simplest elastodynamics, a scalar wave equation (general elastodynamics being two coupled scalar wave equations). We use dimensionless variables throughout, to minimize the number of intrinsic parameters. In the bulk

$$\frac{\partial^2 U}{\partial t^2} = \nabla^2 U \tag{1}$$

where U is the displacement field, t is time, and ∇^2 is the two-dimensional Laplacian operator $\nabla^2 = \partial^2/\partial x^2 + \partial^2/\partial y^2$. We will choose x to be the direction along the fault, and y the direction perpendicular to the fault. As we want to study the intrinsic complexity of the dynamics, we will choose uniform boundary conditions; by studying the most uniform case, which is most likely to give a periodic response, we give a lower bound to the complexity.

The fault is located at $y = 0$, with the boundary condition that the strain is equal to the traction applied on the surface:

$$\left.\frac{\partial U}{\partial y}\right|_{y=0} = \Phi \tag{2}$$

where Φ is the friction. All the nonlinearity in the problem is contained in Φ. We will return to a discussion of Φ shortly; first let's specify the other boundary conditions.

The loading surface is placed parallel to the fault, a distance away. There, the displacement field is moved at a slow steady rate. Without loss of generality, we scale all the lengths in the problem to the distance to this loading surface, so it is located at $y = 1$:

$$\left.\frac{\partial U}{\partial t}\right|_{y=1} = \nu \tag{3}$$

where $\nu \ll 1$ is the slow plate loading rate.

Along the fault direction, we use periodic boundary conditions:

$$U(x + L_x) = U(x) \ . \tag{4}$$

The geometry specified here is illustrated in Figure 1. It remains to specify the friction Φ to complete the description of the model.

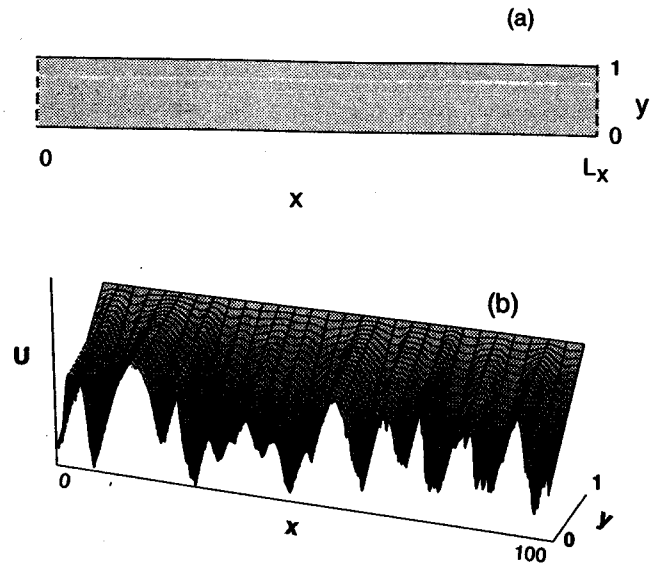

Figure 1. Geometry of the model. (a) The long cylindrical geometry of the space (rectangular, with periodic boundary conditions denoted by dashed lines). (b) The geometry of a typical solution for the displacement U. There is constant displacement along the loading surface at $y = 1$, and irregular displacements along the fault at $y = 0$. The wave equation connects the two boundaries; in this example, where the fault is stuck, the acceleration is zero on the interior, and the Laplacian operator smoothly interpolates between the two boundaries. The x axis is compressed relative to the y axis; the aspect ratio $L_x = 100$ in this example.

The friction Φ is a stick-slip, weakening friction; that is, it resists motion up to a threshold stress value, and then, once sliding begins, it reduces in resistance. In this paper we will use a drastically simplified description of friction, chosen for its relatively simple functional form, because it produces dynamics with a well-defined continuum limit, and because it contains both slip weakening and velocity weakening as end-member cases. Our main justification for departing so severely from more standard formulations of friction is that we are interested in the dynamic behavior at large slip rates, where large frictional heating effects can dramatically alter behavior [*Sibson*, 1973; *Lachenbruch*, 1980; *Shaw*, 1995].

There are four aspects to the friction. First, it is a stick-slip friction, which resists motion up to some threshold value. Second, there is a rapid drop in friction once sliding begins. Third, there is a slower overall weakening which depends on some mixture of slip and slip rate. Fourth, there is a viscous term, which stabilizes the small scales. In a general form, we represent the friction as

$$\Phi = \phi(\frac{\partial S}{\partial t'}, t' \le t) H(\frac{\partial S}{\partial t}) - \eta \nabla_{||}^2 \frac{\partial S}{\partial t} \qquad (5)$$

Here $\frac{\partial S}{\partial t} = \frac{\partial U}{\partial t}\big|_{y=1}$ is the slip rate on the fault, with ϕ depending on the past history of slip. The function H is the antisymmetric step function, with

$$H = \begin{cases} \frac{\hat{\partial S}}{\partial t} & \frac{\partial S}{\partial t} \neq 0; \\ |H| < 1 & \frac{\partial S}{\partial t} = 0 \ . \end{cases} \qquad (6)$$

where $\frac{\hat{\partial S}}{\partial t}$ is the unit vector in the sliding direction. Thus H represents the stick-slip nature of the friction, being multivalued at zero slip rate.

The parameter η is a constant which sets the amount of viscosity, and sets the scale at which the small wavelengths are stabilized. The subscript on the viscous term Laplacian denotes that it is the derivative parallel to the fault, which gives $\nabla_{||}^2 = \partial^2/\partial x^2$ for the geometry considered here in (2) [*Langer and Nakanishi*, 1993].

We choose the particular form for the history dependence of ϕ we take in this paper for two reasons. First is its simplicity. Second, it is motivated by a physical picture of how frictional heating can produce frictional weakening. We will return to the physical motivation; let us first present the mathematical form. We use:

$$\phi = \Phi_0 - \sigma - \frac{\alpha Q}{1 + |\alpha| Q} \qquad (7)$$

The three terms have the following meaning. The first term Φ_0 is a constant which sets the sticking threshold. It turns out to be an irrelevant parameter in the problem, as long as it is large compared to the maximum friction drop, so as to prevent backslipping. This can be seen for the following reason. Since the bulk equations and all the other boundary conditions are linear in U, adding or subtracting a solution of the U field with a constant value of strain on the fault boundary and adding or subtracting that same constant from Φ is also a solution. The additional constant changes the threshold of motion in the opposite direction, which, if there is no backslipping, will be irrelevant. Thus it is only stress drops that matter in the dynamics, not total stress. Φ_0 does affect the heat generated, but that is an effect we will consider here only indirectly, insofar as it feeds back and affects the friction. We will say a bit more about this shortly.

There is one other symmetry in the problem which we have used. The symmetry is the rescaling of the equations of motion, which remain invariant under a rescaling of U, Φ, and ν by the same constant. We have thus, without loss of generality, set the stress change of the last term in (7) to unity, and scaled all the other stresses to this stress change.

For the second term, σ, which represents the rapid drop in friction which occurs in going from sticking to sliding friction, we make a major departure from how usual friction behaves, and make it a time dependent function:

$$\sigma = \begin{cases} \sigma_0 \frac{t - t_s}{\tau} & t - t_s < \tau; \\ \sigma_0 & t - t_s \ge \tau \ . \end{cases} \qquad (8)$$

so that σ increases linearly with time once the fault becomes unstuck, up to a maximum value σ_0 over a timescale τ, and is reset to zero when the fault resticks. The time t_s is measured from the last unsticking and

is reset during an event if the fault resticks and then slips again. This term neglects all the complicated rate and state dependent effects that are observed to accompany the nucleation of slip in laboratory friction experiments [*Dieterich*, 1979, 1992]. We do this for two reasons. First, it allows us to take the limit of the loading rate $\nu \to 0$, so that this parameter is irrelevant to the dynamics, and only sets the timescale between events. Consequently, we have a much more efficient numerical algorithm. Second, many of the aspects of small events do not depend on the details of the nucleation process, and we would like to use as simple a system as is valid for what we are interested in. Our claim is not that this is the most realistic description of nucleation, but, rather, that the properties of the system we are measuring in this paper are insensitive to the details of the nucleation mechanism.

The third term in (7) contains the key dependence on slip and slip rate in the friction, through the variable Q. The variable Q is something like "heat," which accumulates with increasing slip rate and dissipates on a timescale $1/\gamma$:

$$\frac{\partial Q}{\partial t} = -\gamma Q + |\frac{\partial S}{\partial t}| \tag{9}$$

The dissipation with γ gives a simple, physically motivated healing mechanism, which also turns out to give a nice range of properties. An equivalent integral solution of Q:

$$Q(t) = \int_{-\infty}^{t} e^{-\gamma(t-t')} |\frac{\partial S}{\partial t'}| dt' \tag{10}$$

shows that when γ is small compared the inverse rupture timescale of unity, Q is just the slip in an event, while when $\gamma \gg 1$, Q is $1/\gamma$ times the slip rate. (The large γ limit can be seen by noting that $\lim_{\gamma\to\infty} \gamma e^{-\gamma z} = \delta(z)$, where δ is the Dirac delta function.)

The constant α sets the slope of the stress drop with heat Q, with $\alpha > 0$ giving weakening with Q, and $\alpha < 0$ giving strengthening with Q. This parameter plays a crucial role in the problem, as we will see. Because Q is nonnegative, the denominator in (7) only gets larger with Q, eventually saturating the change with αQ.

This third term in (7) , which depends on Q, contains the basic instability in the problem. It is presented here in a way which gives a simple mathematical form while, at the same time, preserving a connection to the physical motivation. The physical picture goes back to *Sibson* [1973], who considered how frictional heating raised the temperature and pressure of pore fluids, thereby decreasing the effective normal stress and thus inducing frictional weakening from frictional heating. *Shaw* [1995] presented a simplified self-consistent dynamics of this effect, showing that one got slip weakening and velocity weakening as end-member limits, depending on whether the dissipation of heat was slow or fast, respectively, compared to the rupture timescale. Earthquakes would be able to dissipate excess pressure with an elastic expansion mode [*Mase and Smith*, 1987], a mode which can happen on the fast rupture timescale. This fast relaxation mechanism suggests values of γ of order unity or larger as the most appropriate values. Thus, a mixture of slip and velocity weakening effects are likely occurring.

Here, we simplify this even further. First, we simplify the heating by ignoring changes in the dynamic friction heat generation, assuming $\Phi_0 \gg 1$, that Φ_0 is large compared to the dynamic stress drop of unity, so that the heat generation in 9) can be taken to be proportional to $|\partial S/\partial t|$ rather than $\Phi_0 \partial S/\partial t$. Then, since we need some nonlinear saturation at high Q, we specify the nonlinear saturation to have the form of the velocity weakening limit for the fully coupled case [*Shaw*, 1995]. Specifying the nonlinear saturation is not a serious constraint, however, as the details of the nonlinear saturation have been shown to be unimportant: an exponential, polynomial, and piecewise linear connection from an initial linear decrease to final constant value were shown to give the same qualitative results in the one-dimensional model [*Shaw*, 1995]. We could, or course, use the fully coupled case; the advantage of this formulation is the simpler form of (9) and (10).

3. Numerical Simulation

To solve the partial differential equation (1), we discretize the bulk into equal finite rectangular blocks, approximating the spatial derivatives with finite differences, and then solve a set of coupled ordinary differential equations in time. The time steps are taken to be small compared to the fastest frequencies in the problem, and are completely resolved in a continuum time sense. It is one of our purposes in this paper to show that a continuum space limit is also achieved.

The numerical procedure is as follows. Starting from any nonsmooth initial condition, the system self-organizes into a statistically steady state, with the attractor being independent of the initial conditions. We begin collecting data after the self-organized state has been reached. The system is loaded continually at the slow loading rate. The fault remains locked while the stress at the fault boundary is less than the frictional strength. When the stress exceeds the sticking friction, the fault begins to move. Depending on how close to threshold the neighbors are, they may or may not come unstuck as the epicentral region begins to slide. The event ends when the whole fault becomes restuck.

One technical point concerns the way the radiated elastic waves are handled. Because we are solving the full inertial dynamics, we have radiated elastic waves. These waves reflect off of the loading boundary at $y = 1$ and travel back to the fault at $y = 0$, telling the fault that it is tied to the loading surface. The waves hitting the fault can either, if it is close enough to failure, unstick it or, if it remains stuck, reflect off of it. Because there is no explicit dissipation in the bulk, the far-field radiation, which consists of the elastic waves which do not go into rearranging the local elastic strain field, and which would travel off to infinity, continues traveling away from the source region. Waiting for these

waves to travel to infinity is obviously impractical, and so they need to be damped out. The waves are damped out between events using the following procedure. Once the whole fault has restuck for some amount of time, we check to see whether the static elastic solution for the current boundary displacement has all the stresses not exceeding the friction strength. This static solution is found by solving the Dirichlet boundary value problem for Laplace's equation (the static scalar elastic equation) with the stuck fault and loading surface as boundaries and, as in the dynamics, periodic boundary conditions along the fault. There are two possibilities. If the static solution has a stress at some point on the fault which exceeds the friction strength, then we know the event is not finished. Hence, we resume the full elastodynamic simulation as before, continuing from where we had interrupted to do the check. If, instead, the static solution indeed has all parts of the fault below the sticking friction strength, then we consider the event done. We then replace the kinetic bulk with the static bulk elastic solution, and analyze the properties of the event that has just been completed. Next, loading is continued until the following event occurs, and the whole process is repeated.

There are three parameters specifying the geometry of the grid we use, all of which can be made to be irrelevant. One physical parameter is the length of the fault L_x (Recall that L_x is in units of $L_y \equiv 1$; see the discussion above 3).) As we will see, if L_x is big enough, in the frictional weakening case the largest events will not break the whole fault length; then L_x does not play any role in any of the statistical measures we examine, and is thus irrelevant.

There are two numerical parameters, both of which can be made irrelevant. They are the grid resolution in the x direction along the fault δ_x, and the grid resolution in the direction perpendicular to the fault δ_y. We have found numerically that when the grid resolution in the perpendicular direction is at least twice the resolution in the fault parallel direction, it is irrelevant; so we use $\delta_y = \delta_x/2$. We will show, in the next section, that δ_x can also be made irrelevant, in the sense that behaviors at the larger scales do not depend on it. We are, at the same time, limited in how resolved we can go. Increasing resolution in the algorithm is expensive numerically. It costs $O(\delta_x^{-3})$, one factor coming from δ_x, one from δ_y, and one from the smaller time steps needed to resolve the smaller spatial scales.

Finally, there is the issue of finite differences and stress concentrations, and accuracy of the numerical simulations. The finite resolution inherent in any numerical treatment implies an inability to resolve changes over very small length scales. Because of the nature of the equation for the bulk, the wave equation, the largest gradients will be generated on the fault boundary. Figure 1b illustrates this for the case when the field is static; when there are dynamic waves, the gradients on the fault propagate into the bulk but do not, however, sharpen. This makes the contribution of the viscous term in the fault friction (5) more clear: it limits the generation of large velocity gradients and therefore large strain and stress gradients from forming on the fault boundary, and therefore from forming in the system. By stabilizing the smallest length scales, it provides a lower scale to the spatial structure that must be resolved, and thus makes it possible for finite numerical resolution to simulate a continuum system.

What about accuracy? The system is, in the complex regime, highly chaotic, so the specifics of a particular long-term configuration are sensitive to the details of the initial conditions (and thus, ultimately, on the resolution). However, as we are only interested in the statistics of the attractor we observe, and not any particular sequence, this kind of sensitivity should not affect the results. The understanding of the results based on the observed attractor rests on the nonlinear dynamics idea of "shadowing"; the idea that the attractor we solve for should follow closely, albeit not exactly, the true attractor of the system. As we have no evidence to the contrary– further temporal and spatial resolution do not alter the results– we interpret the attractor we observe as indeed shadowing the true attractor.

A last point is how we measure how big an event was. The size of an event is given by the moment M, which is the sum of the net slip in an event:

$$M = \int \delta S dx \tag{11}$$

where δS is the slip in an event. The length of the event L is given by the length of the patches which slipped. While most events are simply connected, some events slip in multiple patches.

Results

There are two fundamentally different types of behavior which occur, depending on whether the friction is weakening ($\alpha > 0$) or strengthening ($\alpha < 0$). When it is weakening, beginning from any non-constant initial condition, the system self-organizes into a complex, nonperiodic rough slip distribution, with, when the fault is long enough, events which do not propagate along the whole fault. In contrast, when the friction is strengthening, the system evolves into a smooth slip distribution with events which propagate along the whole fault, no matter how long the fault is. In this strengthening case, any irregularities are associated with small residual slip heterogeneities in the epicentral region left over from the event wrapping around the whole fault; irregularities are not maintained along the whole fault, only at one place, where the rupture wraps around and meets. This is completely different from the weakening case, where the rough slip distribution is maintained along the whole fault. Figure 2 illustrates this difference, with the sequence of slip distributions for a weakening case shown in Figure 2a, and a sequence for a strengthening case shown in Figure 2b. In Figure 2b, we begin from a rough configuration, just to show that even then the strengthening case smoothes the fault. Note in both cases how rapid the approach to the attractor is; the

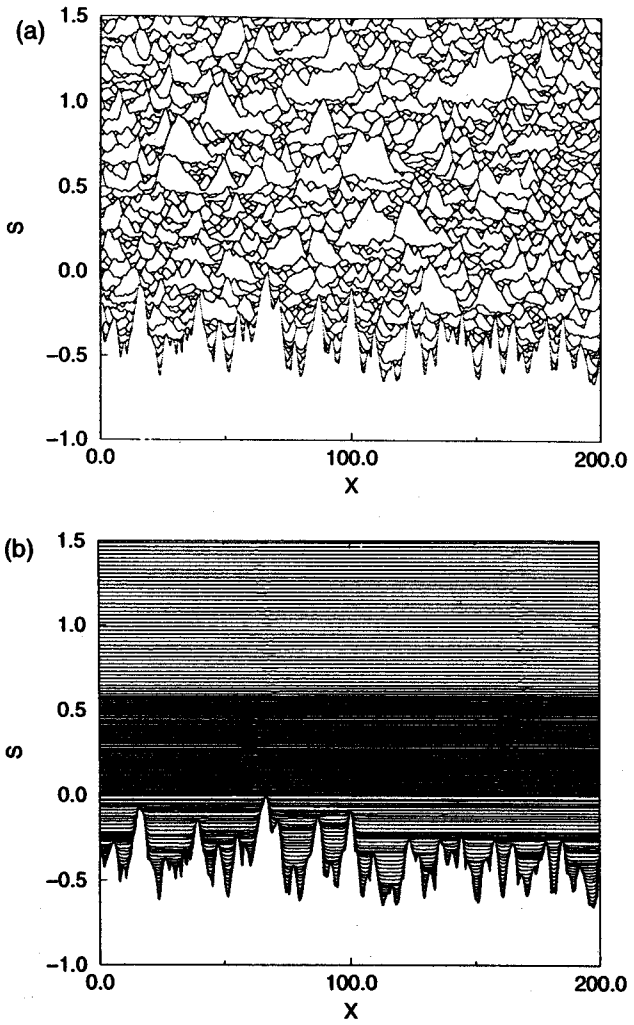

Figure 2. Slip complexity in the weakening case and slip noncomplexity in the strengthening case. The net slip in a sequence of stuck configurations, as a function of position along the fault, is plotted. (a) The complex slip distribution that has developed in the weakening case. Parameter values are $\alpha = 2$, $\gamma = 1$, $\sigma_0 = .03$, $\tau = .1$, $\eta = .005$, $\delta_x = .1$. (b) The smooth slip distribution which develops in the strengthening case; despite beginning from a rough slip initial condition, the fault rapidly smoothes. Parameter values are the same as in Figure 2a, except that α has the opposite sign; so now $\alpha = -2$. To emphasize that the important difference arises from the dynamics, the same initial conditions have been used in both figures.

transition from one type of roughness to another appears almost immediate. The dynamics appear highly dissipative, generally, to motions orthogonal to the attractor, both for the strengthening and weakening cases. We turn our attention to the more interesting weakening case $\alpha > 0$ for the remainder of the paper.

Figure 3 shows a weakening case with a different set of parameters than the weakening shown in Figure 2a, to give a sense of the variations in behavior with parameters in the weakening regime. Figure 3a shows the net slip when it is stuck. Figure 3b shows a different plot of the same sequence of events as in Figure 3a, only now the time at which a given place on the fault moves is marked. This is a more standard plot in seismology, only here we show it for vastly longer times than can be observed seismologically, the equivalent of tens of repeat times for large events, or many thousands of years. We will take the parameter values used in this Figure 3 as the standard ones which will be used in all the figures which follow, unless explicitly noted otherwise. They are $\alpha = 6$, $\gamma = 1$, $\sigma_0 = 0.03$, $\tau = 0.1$, $\eta = 0.005$, $\delta_x = 0.1$ and $L_x = 200$. The first five of these parameters are friction parameters; the last two are geometry parameters. In the weakening case, $\alpha > 0$, when L_x is large enough, the largest events will not propagate around the whole fault, and L_x becomes an irrelevant parameter to the statistics. And,

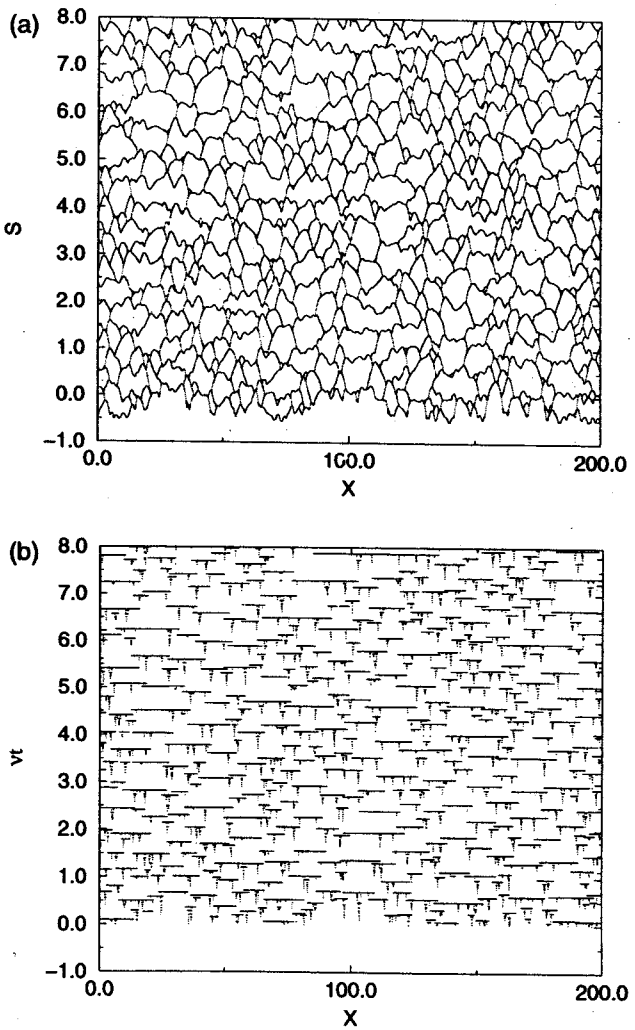

Figure 3. Two different ways of looking at the sequence of events that has developed in a weakening case. (a) The net slip in the stuck configuration, as in Figure 2. (b) The time at which different portions of the fault have slipped. The same sequence of events is shown in Figures 3a and 3b. The parameter values are the same as in Figure 2a, except for α which now has the value $\alpha = 6$. The parameter values used here, $\alpha = 6$, $\gamma = 1$, $\sigma_0 = .03$, $\tau = .1$, $\eta = .005$, and $\delta_x = .1$ are the standard values which will be used in all the following figures, unless noted otherwise.

as we will see shortly, the small numerical discretization length δ_x will also turn out to be irrelevant, for large enough η. The largest events are many times the one physical length in the problem, the crust depth length which has been scaled to unity. What sets the size of the largest events is still not understood. Whether the largest events will be finite or not depends only on α, with the other parameters playing at most quantitative, but not qualitative roles in this issue. And again, when $\alpha > 0$, and when L_x is large enough, the largest events are finite and independent of L_x.

We choose a "standard" set of parameter to see the variations in behavior as one parameter is varied and the others are held fixed. There is nothing particularly special about this choice of parameters being the standard. They represent a reasonable compromise between three sometimes conflicting factors: the values estimated as the most realistic, the numerical tractability, and the values which would provide the clearest illustration of the behavior. The one really important parameter is α; however, I will first discuss all the other parameters.

We chose the parameter $\gamma = 1$ as a standard value based on a desire to study a range of values of γ from small to large, with this being an intermediate value. We will study the whole range of values of γ, and see that, interestingly, it does not change the behaviors we will be examining much. We chose $\sigma_0 = 0.03$ as a standard value as a compromise between the desire to illustrate the behavior of the smallest events, which are best seen with small σ_0, and estimates of the most realistic values of σ_0, which tend to be larger to match constant stress drop observations. The behavior is not very sensitive to this parameter. The choice of $\tau = 0.1$ as a standard value was made to have the value small, so the initial σ stress drop would happen rapidly, but not so small that it would be smaller than the timescale for a signal to propagate along the grid. The behavior was insensitive to a wide range of values of this parameter. We chose $\eta = 0.005$ as a standard value so that it would be big enough to provide a stabilizing effect, but not so big that we lost too much of a scaling regime and the numerics became too inefficient. As long as η was not so large that it quenched the time dependent σ nucleation we used, or so small that it did not regularize the grid, its value did not qualitatively affect the behavior. We chose $\delta_x = 0.1$ as a standard value as a compromise between a desire for the smallest possible value to get the best resolution, and numerical costliness of higher resolution. We will show the independence of the results on this parameter. We chose $L_x = 200$ as a standard value as it is long enough to be an irrelevant parameter, and not so long as to swamp our finite memory and speed capabilities. Our results do not depend on this parameter. For this geometry of $\delta_x = 0.1$, $\delta_y = \delta_x/2$, $L_x = 200$, the corresponding numerical grid was 2000 elements long by 20 elements wide.

The final parameter we must discuss is α. Again, this is the one parameter which makes a big difference in behavior. To the extent that we have selected any special parameter values to obtain a regime of interest, it is α. When α is very small, or α is very large, we get almost all large events, and few small events. For intermediate values of α we get lots of small events. Since we

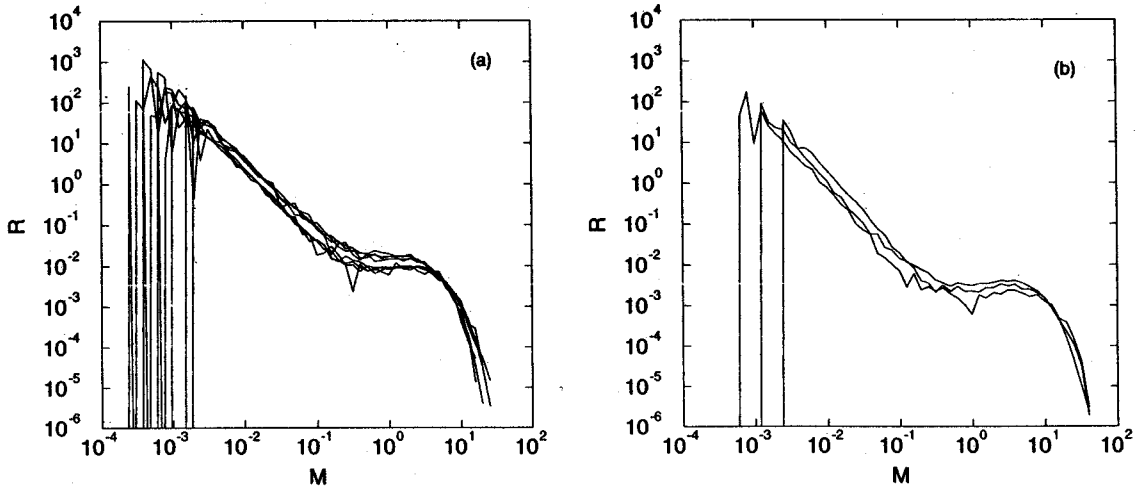

Figure 4. The distribution of sizes of events for different values of the viscosity parameter η and different spatial discretizations δ_x. The rate of events $R(M)$ having moments between M and $M + \delta M$ is plotted. (a) Two different values of η are used, $\eta = .02$ and $\eta = .005$, along with four different values of the spatial discretization, $\delta_x = 1/12,\ 1/10,\ 1/8,\ 1/6$, for a total of eight curves. The four different values of the spatial discretization all collapse onto the same distributions for a given value of η, showing the grid resolution independence of the results. In contrast, the two different values of η give different distributions, with the $\eta = .02$ curves lying above the $\eta = .005$ curves. (b) The viscosity term is absent, $\eta = 0$, and now we can see different values of the discretization give different distributions. Here $\delta_x = 1/10,\ 1/8$, and $1/6$ are plotted with $\delta_x = 1/10$ lying at the bottom, and $\delta_x = 1/6$ lying at the top. Note the similarity between the distributions with different δ_x when $\eta = 0$, and as compared with the distributions with different η when $\eta \neq 0$ in Figure 4a.

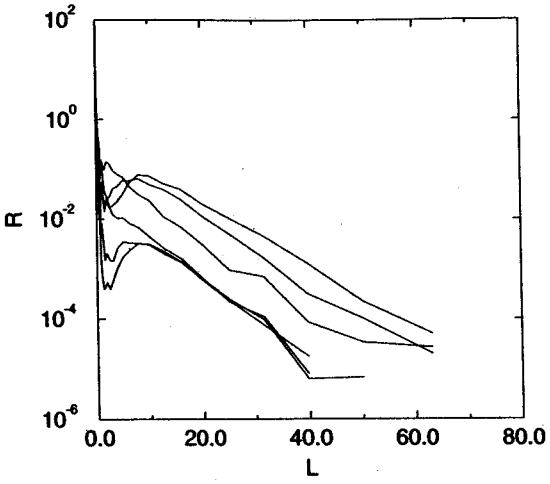

Figure 5. The distribution of lengths of events, for different values of the weakening parameter α. The vertical axis is the rate $R(L)$ of events having length between L and $L+\delta L$, while the horizontal axis is the length L. On this log-linear plot, the linear fit for the largest events shows that they fall off exponentially. The largest events are finite and intrinsic to the dynamics, and do not span the whole length of the system. The values of α used are $\alpha = .5$, 1, 2, 4, 8, and 12, with the curves having the higher values of α being below. Note how weakly the exponential length scale depends on α.

are interested in a range of events, the standard value has been set within this intermediate range. We will further discuss the variation of the behavior with this parameter later. All these preliminaries accomplished, let's see how the model behaves!

First, we show that we obtain events which are independent of grid resolution, and, thus, we have a good continuum solution. As in the 1-D model, the viscosity provides a lower cutoff to the smallest unstable length-scale, which becomes the relevant small length in the self-organization [*Shaw*, 1994]. In the absence of the viscous term, when $\eta = 0$, the grid resolution plays this role. In that case, things are still observed to be qualitatively similar, so that details of the small-scale physics do not appear, qualitatively, to control what happens at the large scales. Figure 4 illustrates this result. Figure 4a plots the distribution of sizes of events for events with different grid resolutions, and with two different values of η, while all the other parameters remain fixed. Four different grid resolutions, $\delta_x = 1/6$, $1/8$, $1/10$, and $1/12$ are used. The two values of η are $\eta = .02$ and .005 . Note that the curves collapse onto two sets, corresponding to the two different values of η, with the collapse being independent of the grid resolution. In contrast, Figure 4b uses the same parameter values, except now with $\eta = 0$. Thus the grid resolution now provides the small scale cutoff. Notice here that the curves no longer collapse. Interestingly, note that the curves for $\eta = 0$ are similar to the curves with $\eta \neq 0$, only now they change with smaller grids as they did with smaller η. This is also seen in the 1-D model [*Shaw*, 1994]. Having shown grid independence for nonzero η, we will restrict our attention from here on to that regime.

Figure 5 shows the distribution of lengths of events for different values of weakening α. Here, the straight line on the log-linear plot shows that the largest events are exponentially distributed. This exponential distribution of the largest events has been seen in experiments on gel analogue fault models [*Rubio and Galeano*, 1994]. It has also been reported as occurring in the 1-D model in the limit of the discretization length becoming large [*de Sousa Vieira*, 1996]. In fact, it is quite ubiquitous, and not at all limited by discretization lengths or dimensionality in the system: in general, the largest events on long enough faults are seen to fall off expo-

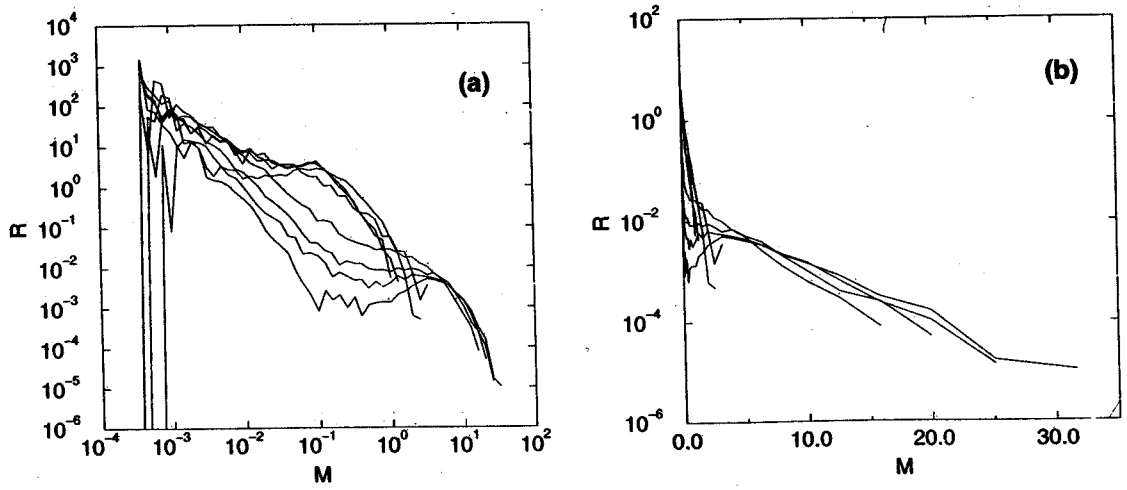

Figure 6. The distribution of sizes of events, for different values of the weakening parameter α. The curves are for the same catalogues of events as in Figure 5. (a) On a log-log scale, with the straight lines on the larger negative α lower curves showing the power law distribution of small events. Note the excess of large events with respect to the extrapolated small event rate. For small negative values of α, the curves converge to the same limiting distribution. (b) The distribution of sizes on a log-linear scale, with the straight line for the largest events showing their exponential distribution. The values of α plotted are $\alpha = .25$, .5, 1, 2, 4, 6, 8, and 12.

nentially in the frictional weakening models. Note, in addition, the very weak dependence of the length scale of the fall off in Figure 5 with α. The length scale does vary some with η, and does have some α dependence; but it varies surprisingly little.

The key parameter affecting the distribution of sizes of events is α. Figure 6a shows the distribution of sizes of events for different values of α, plotted on a log-log scale. We plot the differential rate of events $R(M)$ having events between M and $M + \delta M$; an integral of this distribution would give the cumulative distribution often used for sparse real data. When $\alpha > 0$ there are two regimes of behavior, depending on how large α is. For small α, all the events scale with σ. For larger α, there is a transition to where there are small events which scale with σ, and large events which now scale with the full stress drop of unity. The transition between the two regimes occurs at a critical value of α, where there is the broadest range of scaling. On the log-log plot of Figure 6a, the straight line shows the power law scaling for the small events in the larger α regime. The very smallest events are suppressed below the power law scaling by the viscous term. The large events occur in excess of the extrapolated small event rate. This is consistent with what is observed for real earthquakes on a single fault [*Wesnousky et al.*, 1983; *Singh et al.*, 1983;*Stirling et al.*, 1996]. Averaging over fault systems, which contain many faults of different lengths, gives earthquake distributions which show power laws out to the largest events– the Gutenberg-Richter scaling [*Gutenberg and Richter*, 1954; *Pacheco et al.*, 1992]. Note that the slope of the small events changes somewhat as α changes. Comparing to the real data, the most realistic values of the slopes of small events, and the relative rates of small events to large events, occur for values of α near the critical value. For these intermediate values of α,

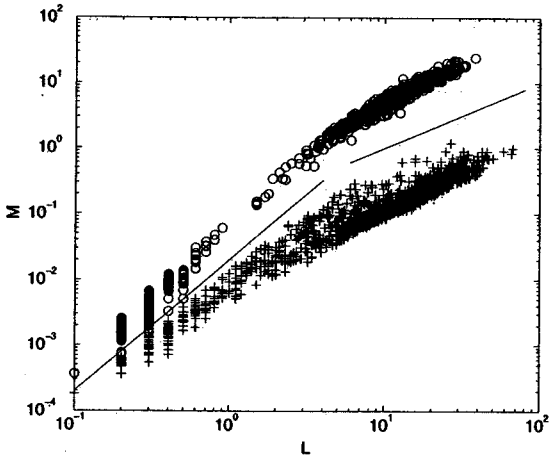

Figure 7. The scaling of moment M with length L of an event. Two different values of α are used, the smallest and largest values shown in Figure 6, with $\alpha = .25$ denoted by crosses and $\alpha = 12$ by the circles. The two solid lines show, for smaller values of L, $M \sim L^2$ scaling, which corresponds to "constant stress drop" scaling in two dimensions, with slip scaling linearly with L, and, for larger values of L, constant slip scaling $M \sim L$.

the friction drop occurs over the scale of slip of a large event. Such a large scale for weakening is obviously unrelated to microscopic friction, and would have to have some other origin; the heat weakening effects we discussed previously would be one possible origin. Other values of α correspond better with other types of fault regimes: negative values of α for faults above and below the seismogenic zone which are in the stable sliding regime, larger values of α for the most developed major faults, like the San Andreas, which have the largest events, and relatively few smaller events. As in the case of the lengths, the largest moments in the model are exponentially distributed; this is shown in Figure 6b, as a straight line on the log-linear plot.

A plot of moment M versus length L of an event shows the scaling of slip with slip zone size. In Figure 7, we plot M as a function of L for a number of events. Two different values of α are shown– the largest and smallest values of α in Figure 6. As in [*Myers et al.*, 1996] we see scaling which is consistent with observations in real earthquakes; for all but the largest events, slip increases linearly with slip zone size, the "constant stress drop" scaling seen in earthquakes [*Scholz*, 1982]. In two dimensions, as we have here, this implies $M \sim L^2$, which is shown by one of the solid line in Figure 7. The other solid line shows constant slip scaling $M \sim L$ for the largest events; again we see consistency with real earthquakes [*Romanowicz*, 1992; *Scholz*, 1994].

Changing the parameter γ changes the relative amount of slip and velocity weakening. It changes things much as changing α does. Figure 8 shows the distribution of sizes as γ is varied. In Figure 8a, we vary γ, keeping α fixed. This looks similar to what is seen when α is varied. In Figure 8b, we vary both α and γ for larger values of γ, showing that the effective weakening for large γ goes as α/γ, as equations (10) and (7) imply. Figures 8a and 8b also show the continuity of behavior across the different relative amounts of slip and velocity weakening.

Changing the size of σ_0 changes things quantitatively, but not qualitatively. For small σ_0, the large events are independent of σ_0. Also for small σ_0, the distribution of small events is independent of σ_0, with only the size of the cutoff of the very smallest events changing. σ_0 sets the scale of the stress drops of the small events. Stress drops of earthquakes are observed to be roughly equal for small and large events, so this suggests that a value of σ_0 close to unity would be the most realistic value. We chose, however, to study smaller values of σ_0 in this paper for two reasons. First, when σ_0 is small, the large events become independent of σ_0, and also the small events scale in a simple way with σ_0; this therefore makes it easier to classify a generic behavior and to study the behavior varying each parameter separately. A second reason for studying smaller values of σ_0 is that it extends the small event scaling regime to smaller magnitudes; since this is a regime which has been the source of some contention, clarifying the behavior in this regime is of particular interest. In any case, larger

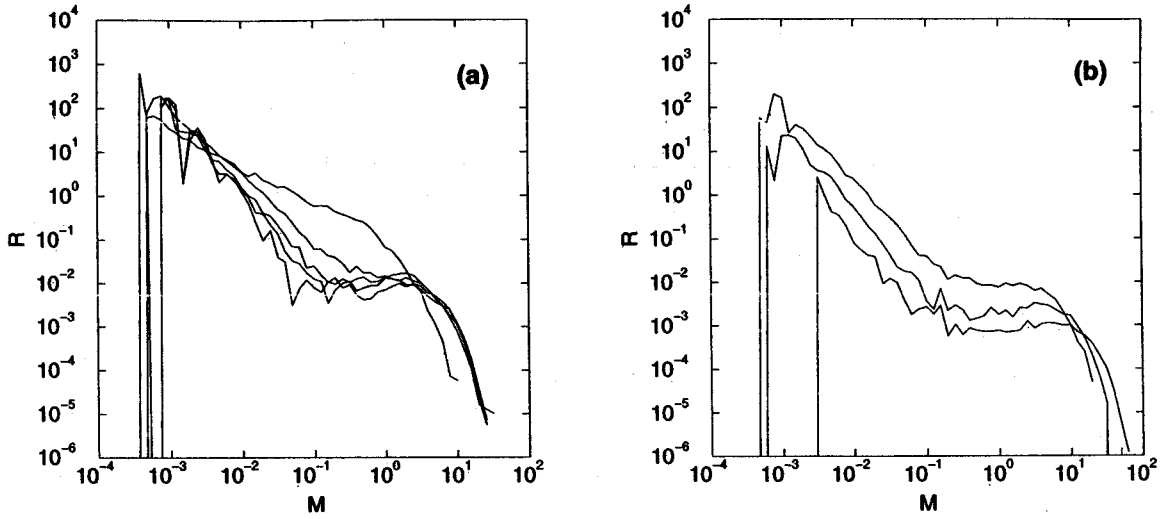

Figure 8. The distribution of sizes of events for different values of the healing parameter γ. (a) Values of $\gamma = 0$, .1, .5, 2, and 10. Note the convergence for small values of γ onto the same pure slip-weakening limiting distribution, while larger values of γ correspond to smaller values of α/γ. (b) Both γ and α are changed, to show the α/γ scaling. The curves here are $\alpha = 6$ $\gamma = 1$, $\alpha = 12$ $\gamma = 2$, and $\alpha = 60$ $\gamma = 10$.

values of σ_0, up to a few tenths, are qualitatively similar in their behavior. The parameter τ is also seen to not effect all but the very smallest events. Of course, if $\sigma_0 = 0$, events which scale with σ_0 will not exist any more. That does not, however, mean that events which scale with σ_0 are an artifact of the particular time dependent nucleation mechanism used here. The relevant part of the friction for obtaining the small events is a rapid initial drop in friction, followed by a much slower overall drop represented by α. (By rapid, we mean rapid as a function of slip, or slip rate, or of some other variable.) The rapid initial drop gives, more generally, nucleation, with the small events scaling with the nucleation stress drop scale. Speculation that the small event complexity we observe is somehow a result of the "zero nucleation size" of the nucleation mechanism used here has not been supported by our observations. For example, a slip weakening nucleation driven with a finite loading rate, a nucleation mechanism which has a finite nucleation size, has also been seen to give behavior similar to that described here [manuscript in preparation].

Different Bulk Geometries

Are the results sensitive to the details of the geometry of the system? *Myers et al.* [1996] considered a crustal plane geometry where the loading occurred throughout the bulk. This gave, instead of the wave equation, equation (1), the Klein-Gordon equation in the bulk:

$$\frac{\partial^2 U}{\partial t^2} = \nabla^2 U + \nu t - U \qquad (12)$$

where the length scale of unity was now set by the coupling strength to the loading surface being unity. The different bulk equations lead to different wave propagation properties in the two models. In the Klein-Gordon equation we have dispersion, as the different wavelengths travel at different speeds, due to the reflection off the bulk loading. In the wave equation model, by contrast, reflections off of the loading happen off of a stiff boundary through a dispersionless bulk. Thus the reflected unloading waves from the loading surface (a real effect in the real Earth, but one which is modeled quite differently in the two models) are very different. Do these differences, and others, show up in the results we have been examining?

Figure 9 shows the distribution of sizes of events using the same friction, but the two different model geometries: the wave equation model from here (equations (1)-(4)) and the Klein-Gordon equation model of *Myers*

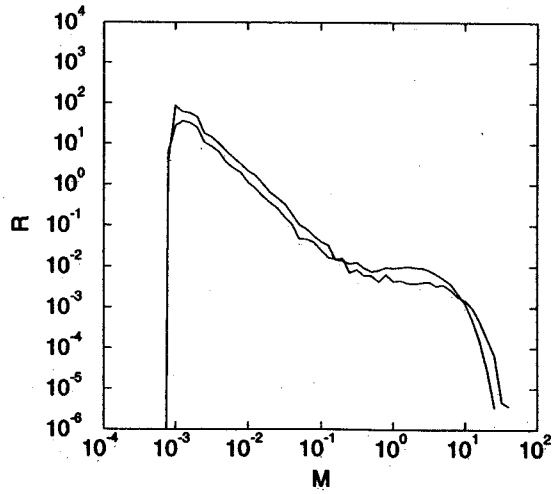

Figure 9. The distribution of sizes of events for the wave equation model described in this paper compared with the distribution of sizes from the Klein-Gordon equation model of *Myers et al.* [1996]. The same frictions are used in both. Note that the two models produce nearly identical distributions.

et al. [1996] (equations (12), (2), and (4)). Observe that the distributions are essentially the same, with only a slight change in the overall scale of events, as the bulk-loaded model is slightly less stiff. The similarities of the behavior extend beyond the distribution of event sizes as well. Remarkably, looking only at the boundary motions on the fault, it appears very difficult to tell the two models apart. This further demonstrates the generic nature of the results in this paper.

4. Conclusion

I have presented a new simple (perhaps the simplest) two-dimensional elastodynamic model of an earthquake fault. It is modeled by the wave equation in the bulk, a uniform frictional boundary, and a parallel loading surface. The model was shown to behave similarly to previous bulk-loaded models which had the Klein-Gordon equation for the bulk. A range of frictions mixing slip and velocity weakening effects was studied, with slip weakening being one end-member case and velocity weakening being the other, and all of them being shown to display a generic type of slip complexity: An exponential distribution of the largest events and, for sufficient weakening, a power law distribution of small events. The addition of a viscous frictional term which stabilized the smallest scales was shown to give a behavior which was independent of grid resolution, thereby indicating that a continuum limit complexity was achieved. This paper extends the class of elastodynamic models, and the class of frictions that have been shown to produce the generic types of slipcomplexity described in this paper. This lends further support to the suggestion that this dynamic complexity may play a role in some aspects of earthquake complexity.

Acknowledgments. This work was supported by NSF grant 94-17700 and USGS grant 1434-95-G-2538.

References

Blanpied, M. L., D. A. Lockner, and J. D. Byerlee, Fault stability inferred from granite sliding experiments at hydrothermal conditions, *Geophys. Res. Lett., 18*, 609, 1991.

Brace, W. F., and J. D. Byerlee, Stick-slip as a mechanism for earthquakes, *Science, 153*, 990, 1966.

Burridge, R., and L. Knopoff, Model and theoretical seismicity, *Bull. Seismol. Soc. Am., 57*, 341, 1967.

Carlson, J. M., and J. S. Langer, Mechanical model of an earthquake fault, *Phys. Rev. A, 40*, 6470, 1989.

Cochard, A., and R. Madariaga, Complexity of seismicity due to highly rate-dependent friction, *J. Geophys. Res., 101*, 25331, 1996.

de Sousa Vieira, M., Exponential distribution in a mechanical model for earthquakes, *Phys. Rev. E, 54*, 5925, 1996.

Dieterich, J. H., Modeling of rock friction, 1, Experimental results and constitutive equations, *J. Geophys. Res., 84*, 2161, 1979.

Dieterich, J. H., Earthquake nucleation on faults with rate and state dependent strength, *Tectonophysics, 211*, 115, 1992.

Gutenberg, B., and C. F. Richter, *Seismicity of the Earth and Related Phenomena*, Princeton Univ. Press, Princeton, N.J., 1954.

Lachenbruch, A., Frictional heating, fluid pressure, and the resistance to fault motion, *J. Geophys. Res., 85*, 6097, 1980.

Langer, J. S., and H. Nakanishi, Models of crack propagation II: two dimensional model with dissipation on the fracture surface, *Phys. Rev. E, 48*, 439, 1993.

Mase, C. W., and L. Smith, Effects of frictional heating on the thermal, hydrologic, and mechanical response of a fault, *J. Geophys. Res., 92*, 6249, 1987.

Myers, C. R., B. E. Shaw, and J. S. Langer, Slip complexity in a crustal plane model of an earthquake fault, *Phys. Rev. Lett., 77*, 972, 1996.

Nielsen, S., L. Knopoff, and A. Tarantola, Model of earthquake recurrence: Role of elastic wave radiation, relaxation of friction and inhomogeneities, *J. Geophys. Res., 100*, 12423, 1995.

Pacheco, J. F., C. H. Scholz, and L. R. Sykes, Changes in frequency size relationship from small to large earthquakes, *Nature, 355*, 71, 1992.

Rice, J. R., and Y. Ben-Zion, Slip complexity in earthquake fault models, *Proc. Natl. Acad. Sci. U.S.A., 93*, 3811, 1996.

Romanowicz, B., Strike-slip earthquakes on quasi-vertical transcurrent faults: inferences for general scaling relations, *Geophys. Res. Lett., 19*, 481, 1992.

Rubio, M., and J. Galeano, Stick-slip dynamics in the relaxation of stresses in a continuous elastic media, *Phys. Rev. Lett., 50*, 1000, 1994.

Scholz, C. H., Scaling laws for large earthquakes: Consequences for physical models, *Bull. Seismol. Soc. Am., 72*, 1, 1982.

Scholz, C. H., Reply to comments on "a reappraisal of large earthquake scaling", *Bull. Seismol. Soc. Am., 84*, 1677, 1994.

Shaw, B. E., Moment spectra in a simple model of an earthquake fault, *Geophys. Res. Lett., 20*, 643, 1993.

Shaw, B. E., Complexity in a spatially uniform continuum fault model, *Geophys. Res. Lett., 21*, 1983, 1994.

Shaw, B. E., Frictional weakening and slip complexity on earthquake faults, *J. Geophys. Res., 100*, 18239, 1995.

Shaw, B. E., J. M. Carlson, and J. S. Langer, Patterns of seismic activity preceding large earthquakes, *J. Geophys. Res., 97*, 479, 1992.

Sibson, R. H., Interactions between temperature and pore fluid pressure during earthquake faulting and a mechanism for partial or total stress relief, *Nature Phys. Sci., 243*, 66, 1973.

Singh, S., M. Rodriguez, and L. Esteva, Statistics of small earthquakes and frequency of occurrence of large earthquakes along the Mexican subduction zone, *Bull. Seismol. Soc. Am., 73*, 1779, 1983.

Stirling, M. W., S. G. Wesnousky, and K. Shimazaki, Fault trace complexity, cumulative slip, and the shape of the magnitude-frequency distribution for strike-slip faults: a global survey, *Geophys. J. Int., 124*, 833, 1996.

Wesnousky, S. G., C. H. Scholz, K. Shimazaki and T. Matsuda, Earthquakes frequency distribution and the mechanics of faulting, *J. Geophys. Res., 88*, 9331, 1983.

B. E. Shaw, Lamont-Doherty Earth Observatory, Columbia University, Palisades, NY 10964. (e-mail: shaw@ldeo.columbia.edu)

(Received December 17, 1996; revised September 16, 1997; accepted September 30, 1997.)